The neutral cysteine protease bleomycin hydrolase is essential for epidermal integrity and bleomycin resistance

DONALD R. SCHWARTZ*, GREGG E. HOMANICS*†, DALE G. HOYT*‡, ED KLEIN§, JOHN ABERNETHY¶, AND JOHN S. LAZO*∥

Departments of *Pharmacology, †Anesthesiology/Critical Care Medicine, and ¶Pathology, and §Division of Laboratory Animal Resources, University of Pittsburgh, Pittsburgh, PA 15261

ABSTRACT The papain superfamily member bleomycin hydrolase (Blmh) is a neutral cysteine protease with structural similarity to a 20S proteasome. Bleomycin (BLM), a clinically used glycopeptide anticancer agent, is deaminated *in vitro* by Blmh. We used gene targeting to generate mice that lack Blmh and demonstrated that Blmh is the sole enzyme required for BLM deamination. Although some Blmh null mice were viable and reproduced, only about 65% of the expected number survived the neonatal period, revealing an important role for Blmh in neonatal survival. Mice lacking Blmh exhibited variably penetrant tail dermatitis that resembled rodent ringtail. The histopathology of the tail dermatitis was similar to skin lesions in humans with pellagra, necrolytic migratory erythema, and acrodermatitis enteropathica. Compared with controls, Blmh null mice were more sensitive to acute BLM lethality and developed pulmonary fibrosis more readily following BLM treatment. Thus, we have established that Blmh is an essential protectant against BLM-induced death and has an important role in neonatal survival and in maintaining epidermal integrity.

Cysteine proteases are a diverse group of important enzymes that include the caspase, calpain, and papain families. Bleomycin hydrolase (Blmh) is a neutral cysteine protease assigned to the papain superfamily based on the conserved amino acid motif surrounding the catalytic cysteine (1). Blmh is expressed in bacteria, yeast, birds, reptiles, and mammals (2–7) with little apparent tissue specificity (7, 8). This ubiquitous distribution suggests an important and as yet undetermined biological role.

The trivial name of Blmh reflects the ability of the enzyme to deaminate and consequently inactivate bleomycin (BLM), a clinically used glycopeptide anticancer agent. Unlike BLM, the metabolite desamido-BLM cleaves DNA poorly and lacks cytotoxicity (9, 10). Yeast strains expressing high levels of Blmh are more resistant to BLM compared with wild-type strains (3). Yeast mutant strains that lack functional Blmh respond to BLM like wild-type cells, suggesting that redundant function(s) may complement the mutated *Blmh* gene (3). Whether redundant cellular activities inactivate BLM or whether orthologues can regulate cell resistance to BLM has not been established in mammals. In BLM-resistant human tumor-cell subclones, 2- to 3-fold more BLM deamidating activity has been observed (11), and treatment with *trans*-epoxysuccinyl-L-leucylamido-(4-guanidino)butane (E-64), a cysteine proteinase specific inhibitor, sensitizes tumors to BLM *in vitro* (12) and *in vivo* (13). Collectively, these data suggest that mammalian Blmh may be an important participant in cellular metabolism of and resistance to BLM.

BLM-induced pulmonary fibrosis has been a significant deterrent to the liberal use of this anticancer agent (14). Low

BLM metabolizing activity has been hypothesized to be the biochemical basis for BLM-induced pulmonary toxicity (10). The factors responsible for other untoward side effects seen in patients treated with BLM, including s.c. toxicity (15) and vascular lesions (16) such as Raynaud's phenomenon (17), are unknown. Recently, we (18) and others (19) reported the genomic organization and chromosomal location (17q11.2) of human *BLMH*, which is a single-copy gene encoding the 455 amino acid Blmh protein. Although the genetic locus of murine *Blmh* is unknown, the region predicted from the human location is one of several mapped for sensitivity to BLM-induced toxicity (20). The development of a mouse model lacking Blmh will help elucidate the natural physiologic function of this highly conserved and ubiquitous cysteine protease and its role in protecting mammals from the toxic actions of BLM.

MATERIALS AND METHODS

Production and Evaluation of Knockout Mice. Strain 129/Ola mouse genomic *Blmh* DNA was isolated from a P1 3 Hit Mouse ES Library (Genome Systems, St. Louis) by screening with PCR primers that corresponded to nucleotides 263–284 and 393–371 of rabbit Blmh cDNA (1). A replacement-type targeting vector (21) was constructed by subcloning genomic DNA (Fig. 1*A*, hatched line) to flank a neomycin phosphotransferase (*neo*) cassette (targeting vector not shown). R1 embryonic stem (ES) cells (22) were transfected by electroporation with the linearized targeting vector and individual G418/ganciclovir-resistant clones were screened for homologous recombination by Southern blot analysis. Ganciclovir was used for negative selection against random vector insertion because the targeting vector contained a thymidine kinase gene located outside of the homologous recombination region. In addition, the targeted allele was differentiated from the wild-type allele by three-primer PCR analysis. The forward primer (p1) for amplification of both the wild-type and targeted allele was 5′-CACTGTAGCTGTACTCACAC-3′. The reverse primers that differentiated the wild-type and targeted allele were 5′-GCGACAGAGTACCATGTAGG-3′ (p2) and 5′-ATTTGTCACGTCCTGCACGACG-3′ (p3), respectively.

Two independently targeted ES cell clones, Bh#127 and Bh#G8 (carrying the targeted mutations *Blmh*^tm1Geh and *Blmh*^tm2Geh, respectively), generated founder chimeric mice that transmitted the targeted allele through the germ line following mating to either C57BL/6J (The Jackson Laboratory) or 129/SvEvTac (Taconic Farms) females. Heterozygous
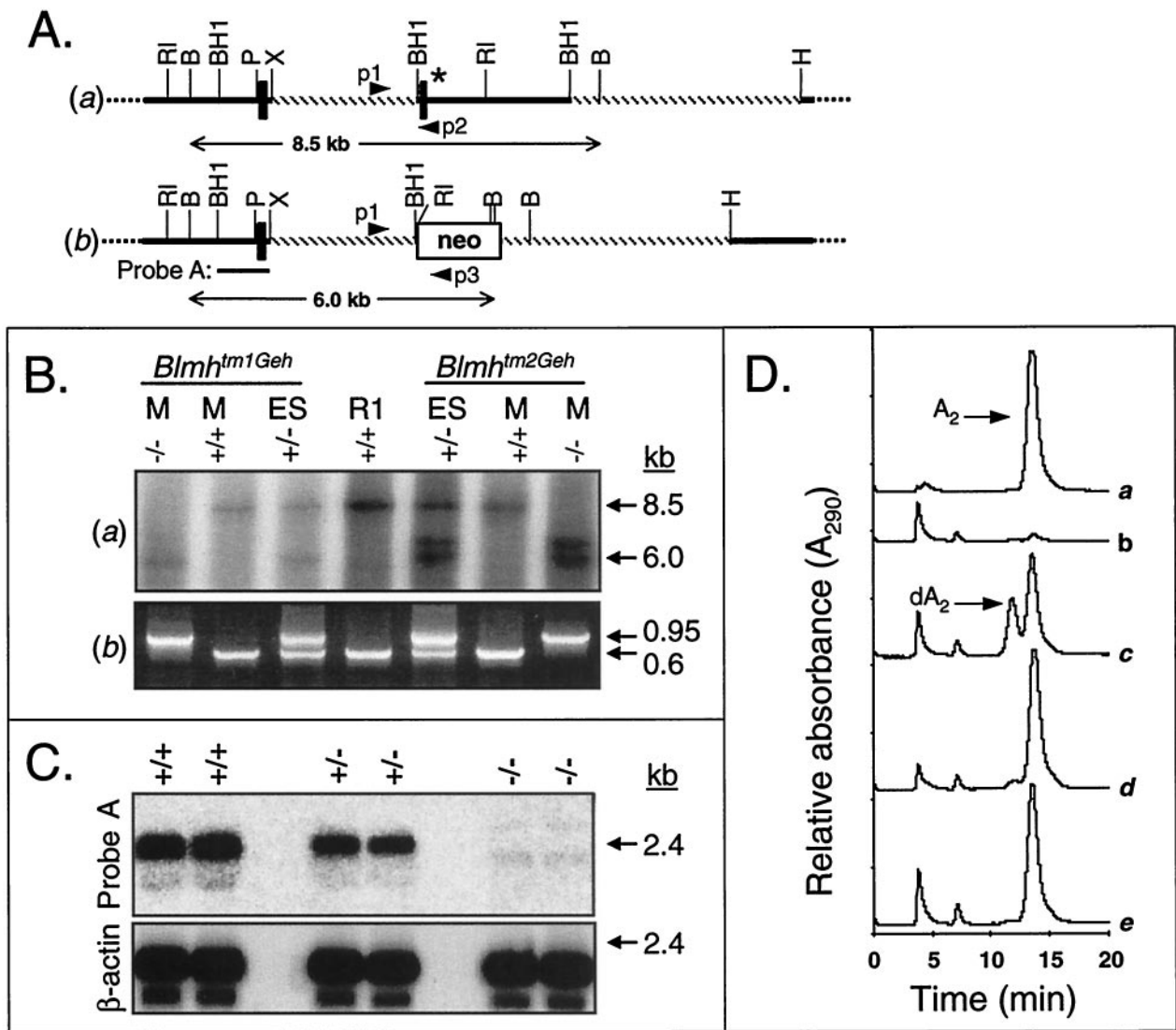

FIG. 1.   Targeted disruption of the *Blmh* gene. (*A*) A replacement vector (not shown) was constructed with two fragments (hatched) of wild-type Blmh genomic DNA (*a*) flanking the neo gene. ∗, Exon 3 encodes (in part) GRCWIF, which is the conserved amino acid sequence surrounding the catalytic cysteine (italicized). (*b*) A targeted *Blmh* allele. PCR primers, p1, p2, and p3; B, *Bgl*II; BH1, *Bam*HI; H, *Hind*III; P, *Pst*I; RI, *Eco*RI; X, *Xba*I. (*B*) Identification of the targeted *Blmh* locus using Southern blot (*a*) and three-primer PCR (*b*) analyses of mouse tail (M) or ES cell DNA. Genomic DNA from heterozygous (+/−) ES cells that contained either *Blmh*tm1Geh or *Blmh*tm2Geh targeted alleles, wild-type parental R1 ES cells (R1), and Bh−/− (−/−), or Bh+/+ (+/+) mice were digested with *Bgl*II and hybridized with probe A (*a*). (*C*) Blmh mRNA expression in embryos using Northern blot analysis. Total RNA from Bh+/+ (+/+), Bh+/− (+/−), and Bh−/− (−/−) embryos was hybridized to probe A (see *A*, *b*) or β-actin cDNA. (*D*) Blmh enzymatic activity in lung homogenates from Bh+/+ and Bh−/− mice was determined by resolving BLM A$_2$ (A$_2$) from its metabolite desamido-BLM A$_2$ (dA$_2$) by reverse-phase HPLC. Representative HPLC tracings are shown from a reaction containing BLM A$_2$ (*a*), Bh+/+ lung homogenates supplemented with either diluent (*b*), substrate (*c*), or substrate and the cysteine protease inhibitor E-64 (*d*), and Bh−/− lung homogenate plus substrate (*e*). Note the lack of desamido-BLM A$_2$ or an alternative metabolite after BLM A$_2$ was exposed to Bh−/− homogenate (*e*).

offspring were intercrossed to produce Blmh wild-type (Bh+/+), heterozygous (Bh+/−), and null (Bh−/−) mice. Because R1 ES cells are a hybrid of strains 129/Sv and 129/SvJ, the genetic background of the mice used in this study was either C57BL/6J × 129/Sv/SvJ (B6, 129) or 129Sv/SvJ × 129/SvEvTac (129). Unless otherwise specified, the results presented were generated from mice carrying the *Blmh*tm1Geh targeted allele. 129-*Blmh*tm1Geh breeding pairs and their litters were fed Prolab Isopro breeder chow (no. 5028, containing 9% fat, 30 international units/g vitamin A; T. R. Last, Pittsburgh). All other mice were fed Prolab Isopro chow (no. 3000, containing 6% fat, 19 international units/g vitamin A, T. R. Last). Weight of mice at weaning was evaluated using a Student's *t* test.

Northern Blot and Blmh Enzymatic Activity Assays. Total RNA for Northern blot analysis was isolated from embryonic

day 16–18 whole embryos using TRIzol reagent (Life Technologies). Blmh mRNA was detected with probe A (see Fig. 1*A*, *b*). RNA loading (≈15 μg per lane) and integrity was monitored with a human β-actin cDNA probe (CLONTECH). Blmh enzymatic activity was assayed in postmicrosomal supernatant fractions by resolving bleomycin A$_2$ (BLM A$_2$) from the desamido-BLM A$_2$ metabolite by HPLC as previously described (23).

BLM Treatment and Hydroxyproline Assay. Weight-matched female 10- to 12-week-old mice from both genetic backgrounds were used. Mice received BLM (10–100 mg/kg; Sigma) or vehicle (saline) as a constant s.c. infusion delivered by mini-osmotic pump (model 2001, Alza) as described (24). Six weeks after initiation of BLM treatment, mice were deeply anesthetized by methoxyflurane (Pitman–Moore, Mundelein, IN) and the thoracic cavity was exposed. The right lung was

Table 1. Genotype of weanling mice and embryos

| Developmental stage | Bkgd | Blmh genotype distribution | | | | | | n | X^* | $P^\dagger$ |
| | | +/+ | | +/− | | −/− | | | | |
		E	O	E	O	E	O			
Weanlings	B6,129	148	175	295	311	148	104	590	10.4	0.0056
	129	70	97	140	147	70	35	279	16.2	0.0003
Embryos	B6,129	8	5	15	18	8	7	30	1.85	NS

Bkgd, genetic background; E, expected (assuming a 1:2:1 Mendelian distribution) number of mice; O, observed number of mice; NS, not significant.
*χ^2 satistic.
†Significant at a confidence interval of 0.95.

removed and its hydroxyproline content was determined as described (10). Data were analyzed by Student's *t* test.

Exposure of Mice to High and Low Relative Humidity. Adult Bh−/− and Bh+/+ littermates lacking tail dermatitis were placed in cages ($n \leq 4$) and fed chow and water ad lib. The cages were placed in two sealed clear Plexiglas (Commercial Plastics and Supply, Pittsburgh) chambers ($60 \times 82 \times 39$ cm) with continuous air circulation of 10 liters/min. One chamber was maintained at high humidity by circulating air that was percolated through reservoirs containing sterile deionized H_2O. A second chamber was maintained at low humidity by inclusion of Drierite (Fisher Scientific) in the chamber. Humidity and temperature were recorded daily with a dual hygrometer/thermometer (VWR Scientific).

Histology. At the time of necropsy, tail biopsies were submerged in 4% paraformaldehyde in 0.1 M sodium phosphate (pH 7.2) overnight at 4°C. Fixed tails were decalcified in 10% nitric acid for 6 hr at room temperature, and 2- to 3-mm-thick pieces were paraffin embedded, sectioned at 6 μm, and stained with hematoxylin and eosin. Other necropsy tissue was treated as above without decalcification.

RESULTS

Production and Molecular Characterization of Mice. Homologous recombination in murine ES cells was used to abrogate *Blmh* gene expression (Fig. 1*A*). The targeting vector was designed to replace exon 3 and 3.4 kb of flanking DNA with a neo gene. Deletion of exon 3 removed the critically important catalytic cysteine. Of 475 G418/ganciclovir-resistant ES cell clones analyzed, six had restriction fragment length polymorphisms indicative of gene targeting at the *Blmh* locus, and two (Bh#127 and Bh#G8 containing *Blmh*[tm1Geh] and *Blmh*[tm2Geh] targeted alleles, respectively) were chosen for further analysis. Probe A (see Fig. 1*A*, *b*) hybridized to the 8.5-kb *Bgl*II fragment from the wild-type allele found in R1 parental ES cells and to a 6.0-kb *Bgl*II fragment from the *Blmh*[tm1Geh] and *Blmh*[tm2Geh] targeted alleles (Fig. 1*B*, *a*). Interestingly, an additional 6.5-kb band hybridized to probe A from the *Blmh*[tm2Geh] allele (Fig. 1*B*, *a*). After extensive Southern blot analysis we have determined that the targeting event in *Blmh*[tm2Geh] resulted in duplication of both the homologous recombination region of the targeting vector and a small fragment of DNA ($\approx$1.5 kb) surrounding exon 2. We have also detected two copies of the targeting construct integrated at the *Blmh* locus in *Blmh*[tm1Geh]. Importantly, following extensive characterization of the targeted alleles with several restriction enzyme/probe combinations, we have concluded that there are no alterations outside of the region of homologous recombination (data not shown). Both ES cell clones described above produced chimeric founder mice that passed the targeted allele through the germ line. Three-primer PCR analysis demonstrated that both targeted alleles lacked the 3.4-kb *Blmh* genomic region, which contains exon 3 and hybridizes to primer p2 (see Fig. 1*A*). *Blmh* null alleles, therefore, lack the

$\approx$650-bp wild-type PCR amplicon that was synthesized between primers p1 and p2 (Fig. 1*B*, *b*).

Importantly, we established in Bh−/− mice that the *Blmh*[tm1Geh] and *Blmh*[tm2Geh] targeted alleles were nonfunctional (i.e., true null alleles) by absence of wild-type Blmh mRNA (Fig. 1*C*), lack of Blmh protein (by Western blot analysis, data not shown), and failure of tissue homogenates to metabolize BLM (Fig. 1*D*). Pulmonary homogenates from Bh+/+ and Bh−/− mice were tested for their ability to metabolize BLM A_2 to its metabolite desamido-BLM A_2. BLM A_2 and desamido-BLM A_2 were resolved by reverse-phase HPLC and clearly detected by absorbance at 290 nm (Fig. 1*D*); compare HPLC traces from reactions with only substrate (a), only homogenate (b), or wild-type homogenate incubated with substrate (c). Pulmonary homogenates from Bh+/+ mice metabolized >30% of the parent compound to desamido-BLM A_2 (Fig. 1*D*, *c*). The cysteine protease inhibitor E-64 prevented the metabolism of BLM A_2 (Fig. 1*D*, *d*), suggesting that production of desamido-BLM A_2 by Bh+/+ homogenate was due to cysteine protease enzymatic activities. Bh−/− lung and liver (data not shown) homogenates, importantly, did not metabolize BLM A_2, even after 12 hr at 37°C (Fig. 1*D*, *e*). Significantly, no alternate BLM metabolites appeared after long exposure to Bh−/− lung homogenates (Fig. 1*D*, *e*). This finding demonstrates that only Blmh is capable of deaminating BLM in mammalian cells and that *Blmh* is a single-copy gene in mice. We conclude, therefore, that the strategy employed for targeted disruption of the *Blmh* gene resulted in a verifiable *Blmh* null allele and that cytosolic deamination of BLM cannot be replaced by a redundant mechanism in Bh−/− mammalian cells.

Neonatal Lethality, Abnormal Epidermis of the Tail, and Reduced Body Weight. Approximately 64% (139) of the expected number (218) of null animals (from both backgrounds) survived to weaning (Table 1). The distribution of genotypes was significantly different from the expected 1:2:1 Medelian distribution. A similar trend was observed for Bh−/− mice having the *Blmh*[tm2Geh] allele, although the number of mice available in our secondary mouse colony limited the power of our statistical analysis (data not shown). To assess whether or not the Bh−/− deaths occurred *in utero*, we genotyped DNA derived from whole embryos (embryonic day 14–18). All embryos appeared viable and no embryo reabsorptions were observed in three litters ($n = 30$ embryos). The genotypes did not differ significantly from a 1:2:1 Mendelian distribution (Table 1). Therefore, $\approx$36% of the Bh−/− pups died as neonates; the cause of death has not been determined. Those Bh−/− mice that survived the neonatal period were healthy and fertile.

Most newborn Blmh null mice appeared normal except for unusual dermatopathy presenting initially as a mild ichthyotic-like appearance with generalized scaling and sloughing of the skin over the entire body. At about the time of expression of pigment within hair follicles ($\approx$7–10 days), the scaling resolved except on the tail. When Bh−/− pups were about 5- to 7-days old, annular constrictions began to appear on the tail (Fig. 2*A*)
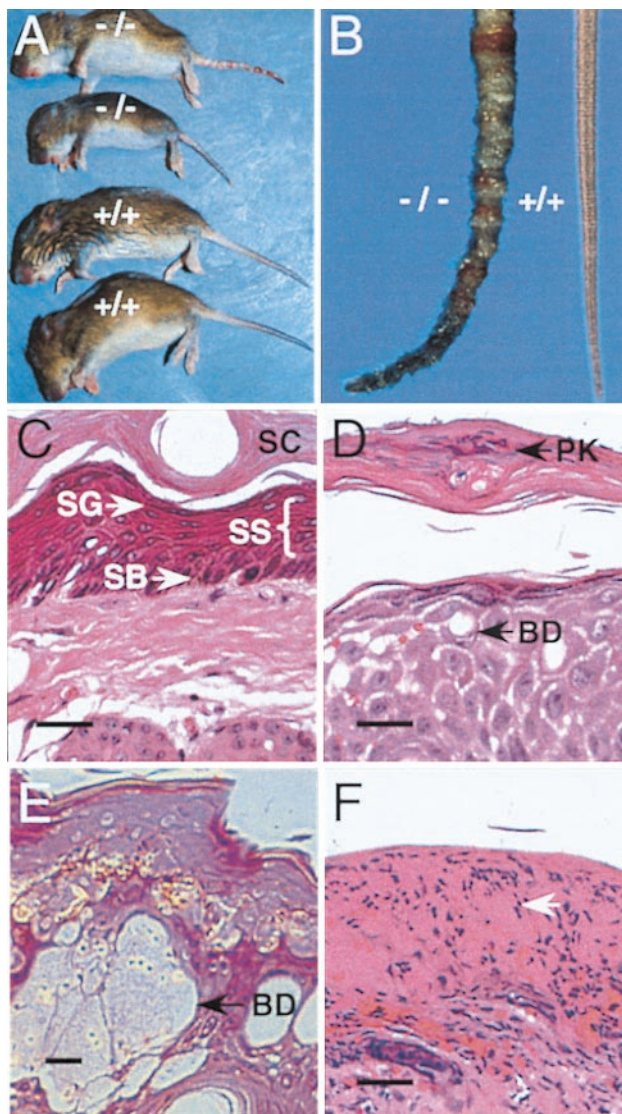
FIG. 2. Gross appearance and histopathology of tail dermatitis on Blmh null mice. (A) The gross appearance of 18-day-old wild-type (+/+) and Blmh null (−/−) littermates. Dermatitis is apparent only on the tail of Blmh null pups. (B) Tails from adult wild-type (+/+) and Blmh null (−/−) mice. (C–F) Hematoxylin- and eosin-stained cross sections (6 μm) of tail biopsies from Bh+/+ (C) and Bh−/− (D–F) mice. The arrowheads in D and E identify ballooning degeneration (BD) of the stratum spinosum. (F) Full thickness necrosis and abundant neutrophil infiltrate (arrow), from a Blmh null mouse afflicted with severe dermatitis. SB, stratum basale; SC, stratum corneum; SG, stratum granulosum; SS, stratum spinosum; PK, parakeratosis. (Bars = 25 μm.)

followed by swelling (dermatitis), erythmatosis, and necrosis and autoamputation of the tip. The gross tail lesions were found exclusively on Bh−/− mice, regardless of genetic background (Fig. 2A). The penetrence and the severity of the lesions were variable. Frequently, the lesions resolved by weaning. Both male and female Bh−/− mice were housed individually without resolution of the tail pathology (data not shown), indicating that the lesions were not caused by aggressive behavior. No lesions were observed in weanlings or adults on other areas of exposed skin (e.g., ears or feet), or on shaved backs of adults exposed to ambient laboratory light 24 hr per day (data not shown), which eliminated visible light as an etiologic agent. The gross lesions were strikingly similar to rodent ringtail, a condition first described >40 years ago (25), which has an elusive etiology. Similar to ringtail, the tail

dermatitis in Bh−/− mice included thickening of the epidermis (parakeratotic hyperkeratosis and acanthosis), areas of necrosis, and neutrophil infiltrate (Fig. 2 D–F). Unlike ringtail, ballooning degeneration of the upper stratum spinosum and pallor (Fig. 2E) were observed in some Bh−/− tails. There was no evidence of underlying angitis or vascular thrombosis. In the most severe cases (Fig. 2F), a thick hardened exudate or inflammatory scale-crust was present on the tail surface with full-thickness epidermal necrosis and an abundant epidermal neutrophil infiltrate.

Rodent ringtail has been reported to be induced by low (<40%) relative humidity (25). Our mice were housed in a facility that had centrally controlled (>40%) relative humidity, however, and there was no evidence of ringtail in any other mouse colony or strain within the facility. Nonetheless, we monitored the humidity directly in our mouse quarters and found that during the coldest ambient weather (roughly <10°C), the relative humidity transiently dropped as low as 25%. Therefore, we tested the hypothesis that tail lesions expressed only on Bh−/− mice were induced by low relative humidity. Wild-type and Bh−/− littermates (8–10 weeks), with no evidence of dermatitis throughout their life, were placed in chambers that received 10 liters/min of either humidified or arid air for 20 days. The mean relative humidity in the humid and dry chambers was 80.1 ± 1.2% and 20.7 ± 0.6%, respectively. Only Bh−/− mice in the dry atmosphere developed tail dermatitis (Fig. 3). Histologically, low-humidity-induced tail lesions on Bh−/− mice had features also present in spontaneous tail lesions, namely parakeratotic hyperkeratosis (data not shown). Rodent ringtail in rats has been alleviated by changing the source of fat and vitamin A (26). Switching our 129-*Blmh*^{tm1Geh} breeding colony from normal chow to high-fat breeder chow did not alter the expression, severity, or frequency of observed dermatitis, irrespective of the ambient humidity (data not shown).

A general histopathological evaluation of multiple tissues from Bh−/− and Bh+/+ littermates was performed. Bh−/− mice replete with conspicuous tail dermatitis lacked abnormalities in other examined tissues (data not shown). Bh−/− mice did frequently appear smaller than their wild-type (see Fig. 2A) or heterozygous littermates. Body weight at the time female pups were weaned (19–22 days after birth) for 129-*Blmh*^{tm1Geh} litters (between 5 and 8 surviving pups) was 10.95 ± 0.53 g (n = 13) for Bh+/+ mice and 9.46 ± 0.74 g (n = 7) for Bh−/− mice (P = 0.05).

In Vivo Response to BLM. Adult wild-type and null mice were treated s.c. with BLM for 7 days to determine if Bh−/− mice were more sensitive to the drug's toxic effects. Blmh deficiency clearly sensitized mice to the toxic effects of BLM because all Bh−/− mice (n = 8) exposed to 100 mg/kg BLM died on day 9–10 following pump implantation (Table 2). In contrast, 1 of 13 Bh+/+ mice died after being treated similarly (Table 2). BLM-induced lethality in Bh−/− mice (1 of 4) was also observed after 50 mg/kg (data not shown). The BLM-resistant Bh+/+ mice survived beyond 6 weeks post-drug delivery, which is consistent with previous reports (24). Necropsy of two Bh−/− mice that received 100 mg/kg BLM revealed evidence of lesions in bone marrow and gut. Within medullary regions of bone, there was a general loss of normal hematopoetic cellularity, especially erythroid components. The marrow appeared hypercellular, which is associated with the infiltration of large numbers of mature neutrophilic inflammatory cells. Multifocal regions of mild gastritis with associated superficial mucosal ulceration and hemorrhage were also seen, which could have been exacerbated by anorexia. We conclude that mammalian Blmh protects whole organisms from BLM.

Next, we examined the sensitivity of Bh−/− mice to the pulmonary fibrotic effects of BLM. The extreme sensitivity of Bh−/− mice to the acute toxicity of BLM, however, restricted
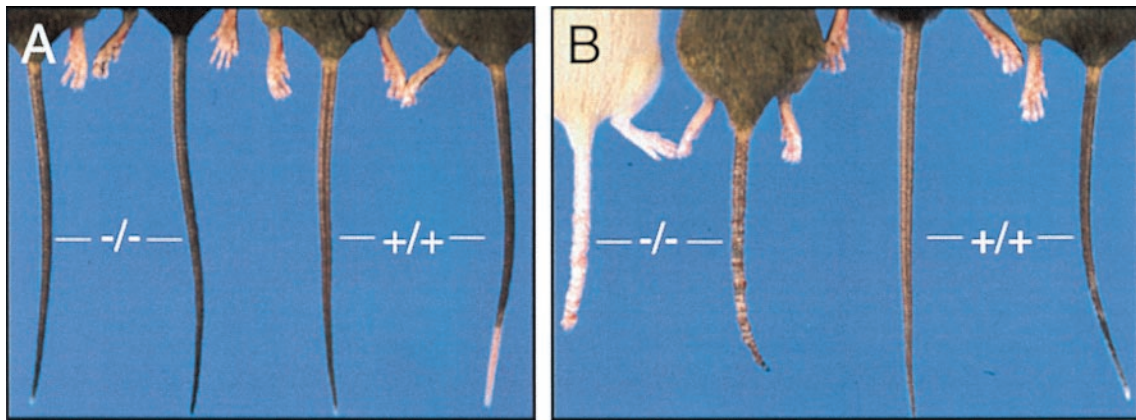
FIG. 3.   Low-humidity-induced dermatitis in Bh−/− mice following 20 days in humidity-controlled chambers. Gross appearance of Blmh null (−/−) and wild-type (+/+) littermates following exposure to either high (*A*; 80.1 ± 1.2%) or low (*B*; 20.7 ± 0.6%) relative humidity.

our study to nonlethal, low doses of BLM. We found Bh−/− mice reproducibly had less basal hydroxyproline, a biochemical marker of collagen (27), than Bh+/+ mice (Fig. 4). This may reflect a smaller lung size in the null mice. As expected, Bh+/+ mice had similar levels of hydroxyproline after low-dose BLM treatment compared with saline (Fig. 4). In contrast, Bh−/− mice treated with 25 mg/kg BLM reproducibly had significantly elevated hydroxyproline levels (30 ± 0.13%; $P < 0.05$) due to collagen deposition during fibrosis. Our data were appropriately normalized to total lung, rather than wet tissue weight or total protein, as has been established by others (28, 29). The magnitude of the hydroxyproline increase in the Bh−/− mice was consistent with our expectations at these normally nontoxic doses. Thus, the absence of Blmh significantly increased BLM-induced pulmonary fibrosis.

DISCUSSION

The creation of mice that specifically and completely lack detectable Blmh enzymatic activity unambiguously demonstrated a unique and nonredundant role for Blmh in BLM metabolism. Moreover, Bh−/− mice were hypersensitive to the deleterious effects of BLM because doses that were without effect in Bh+/+ mice elicited either pulmonary fibrosis (25 mg/kg) or lethality (50 or 100 mg/kg) in Bh−/− mice. As a result, we have unequivocally demonstrated a role for Blmh in protecting mammalian tissue and animals from BLM-induced toxicity. Development of a mammalian model that lacks BLM deaminating activity may greatly facilitate research aimed at understanding and preventing BLM-induced pulmonary fibrosis.

Bh−/− mice had additional phenotypic abnormalities. Approximately 36% of Bh−/− mice died as neonates by an unknown mechanism. Viable Bh−/− neonates frequently presented with tail dermatitis that was greatly exacerbated by dry air. The gross anatomical features of the dermatitis resembled rodent ringtail, which has been observed in rats,

mice, and the white-tailed hamster (25, 30–32), and has been associated with arid conditions (25, 32). The ringtail-like features in the Bh−/− mice include: sloughing skin, annular constrictions, erythmatosis, crust formation, necrosis, and autoamputation (Fig. 2). The specific combination of histopathological changes observed in the Bh−/− tail, namely ballooning degeneration of the upper stratum spinosum and pallor, together with typical markers of rodent ringtail such as hyperkeratosic parakeratosis, neutrophilic infiltrate, and necrosis, have not been reported previously (26, 33). Instead, this unique combination of histomorphological features in Bh−/− tail lesions was similar to descriptions of human skin lesions associated with pellagra, necrolytic migratory erythema (glucagonoma), and acrodermatitis enteropathica (34). These human conditions result from disparate nutritional deficiencies (34). Interestingly, fat, fatty acid, and vitamin B (except B_2) nutritional deficiencies have been suggested as etiologic factors in ringtail (32). The Blmh null mice, therefore, may provide a unique model to probe the as yet unknown molecular mechanism(s) responsible for these lesions.

The Blmh null phenotype has been observed in two independently targeted Blmh null alleles. We cannot rule out the remote possibility that the strategy used to create the Blmh null alleles also disrupted other gene(s), although no other ORF has been detected in the 3.4-kb deleted region (unpub-

Table 2.   BLM-induced lethality in Blmh null mice

Genotype	Allele	Genetic background	*n*	No. died	TOD
Bh+/+	Wild type	C57BL/6J	3	0	—
	Wild type	129/SvEvTac	3	0	—
	Wild type	B6,129	6	1	14
	Wild type	129	1	0	—
Bh−/−	Blmh[tm1Geh]	B6,129	4	4	9.5
	Blmh[tm1Geh]	129	2	2	9
	Blmh[tm2Geh]	B6,129	2	2	9

BLM (100 mg/kg) was delivered (for 7 days) by continuous infusion from a mini-osmotic pump implanted s.c. in the middorsum. TOD, time of death (in days) from pump implantation.
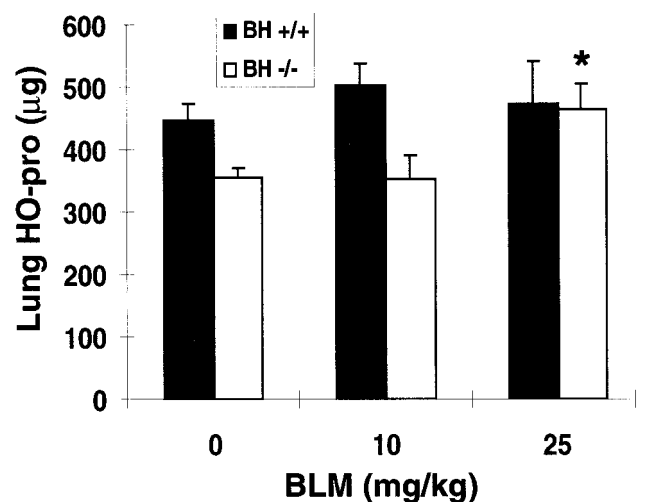

FIG. 4.   Hydroxyproline (HO-pro) content of right lung 6 weeks after a 7-day continuous s.c. infusion of BLM or saline. Bh+/+ and Bh−/− mice received saline (*n* = 4) or BLM (10 mg/kg, *n* = 4; or 25 mg/kg, *n* = 5). Results are shown as mean ± SEM. ∗, $P < 0.05$, Student's *t* test: BLM vs. saline groups of Bh−/− mice.

lished data). Importantly, however, our data suggest that Blmh ablation was both necessary and sufficient for the consequent phenotype.

1. Sebti, S. M., Mignano, J. E., Jani, J. P., Srimatkandada, S. & Lazo, J. S. (1989) *Biochemistry* **28**, 6544–6548.
2. Chapot-Chartier, M. P., Rul, F., Nardi, M. & Gripon, J. C. (1994) *Eur. J. Biochem.* **224**, 497–506.
3. Kambouris, N. G., Burke, D. J. & Creutz, C. E. (1992) *J. Biol. Chem.* **267**, 21570–21576.
4. Adachi, H., Tsujimoto, M., Fukasawa, M., Sato, Y., Arai, H., Inoue, K. & Nishimura, T. (1997) *Eur. J. Biochem.* **245**, 283–288.
5. Nishimura, C., Tanaka, N., Suzuki, H. & Tanaka, N. (1987) *Biochemistry 26*, 1574–1578.
6. Takeda, A., Higuchi, D., Yamamoto, T., Nakamura, Y., Masuda, Y., Hirabayashi, T. & Nakaya, K. (1996) *J. Biochem.* **119**, 29–36.
7. Brömme, D., Rossi, A. B., Smeekens, S. P., Anderson, D. C. & Payan, D. G. (1996) *Biochemistry* **35**, 6706–6714.
8. Ferrando, A. A., Velasco, G., Campo, E. & Lopez-Otin, C. (1996) *Cancer Res.* **56**, 1746–1750.
9. Lazo, J. S., Braun, I. D., Meandzija, B., Kennedy, K. A., Pham, E. T. & Smaldone, L. F. (1985) *Cancer Res.* **45**, 2103–2109.
10. Lazo, J. S. & Humphreys, C. J. (1983) *Proc. Natl. Acad. Sci. USA* **80**, 3064–3068.
11. Lazo, J. S., Braun, I. D., Labaree, D. C., Schisselbauer, J. C., Meandzija, B., Newman, R. A. & Kennedy, K. A. (1989) *Cancer Res.* **49**, 185–190.
12. Sebti, S. M., Jani, J. P., Gorelik, E. & Lazo, J. S. (1991) *Cancer Res.* **51**, 227–232.
13. Jani, J. P., Mistry, J. S., Morris, G., Davies, P., Lazo, J. S. & Sebti, S. M. (1992) *Cancer Res.* **52**, 2931–2937.
14. Lazo, J. S. & Chabner, B. A. (1996) in *Cancer Chemotherapy and Biotherapy: Principles and Practice*, eds. Chabner, B. A. & Longo, D. L. (Lippincott-Raven, Philadelphia), pp. 379–394.
15. Strauman, J. J., Rosen, N. L., Soifer, I. & Wiernik, P. H. (1985) *Cancer Treat. Reports* **69**, 561–562.
16. Burkhardt, A., Holtje, W. J. & Gebbers, J. O. (1976) *Virchows Arch. A Path. and Histol.* **372**, 227–236.
17. Vogelzang, N. J., Torkelson, J. L. & Kennedy, B. J. (1985) *Cancer* **56**, 2765–2770.
18. Montoya, S. E., Ferrell, R. E. & Lazo, J. S. (1997) *Cancer Res.* **57**, 4191–4195.
19. Ferrando, A., Pendas, A., Elena, L., Velasco, G., Lidereau, R. & Lopez-Otin, C. (1997) *J. Biol. Chem.* **272**, 33298–33304.
20. Haston, C. K. & Travis, E. L. (1997) *Cancer Res.* **57**, 5286–5291.
21. Mansour, S. L., Thomas, K. R., Deng, C. & Capecchi, M. R. (1988) *Nature (London)* **336**, 348–353.
22. Nagy, A., Cocza, E., Merenties Diaz, E., Prideaux, V. R., Ivanyi, E., Markkula, M. & Rossant, J. (1990) *Development (Cambridge, U.K.)* **110**, 815–821.
23. Sebti, S. M., DeLeon, J. C. & Lazo, J. S. (1987) *Biochemistry* **26**, 4213–4219.
24. Harrison, J., J. H. & Lazo, J. S. (1987) *J. Pharmacol. Exp. Ther.* **243**, 1185–1194.
25. Njaa, L. R., Utne, F. & Braekkan, O. R. (1957) *Nature (London)* **180**, 290–291.
26. Dikshit, P. K. & Sriramachari, S. (1958) *Nature (London)* **181**, 63–64.
27. Hoyt, D. & Lazo, J. S. (1997) in *Comprehensive Toxicology*, eds. Sipes, I. G., McQueen, C. A. & Gandolfi, A. J. (Pergamon, New York), pp. 543–553.
28. Witschi, H. P. (1975) *Essays Toxicol.* **6**, 120–191.
29. Witschi, H. P., Tryka, A. F. & Lindenschmidt, R. C. (1985) *Fundam. Appl. Tox.* **5**, 240–250.
30. Nelson, J. (1960) *J. Med. Education* **35**, 34–43.
31. Ellison, G. T. & Westlin-van Aarde, L. M. (1990) *Lab. Anim.* **24**, 205–206.
32. Stuhlman, R. & Wagner, J. (1971) *Lab. Anim. Sci.* **21**, 585–587.
33. Koopman, J. P., Van Der Logt, J. M., Mullink, J. A., Heessen, F. A., Stadhouders, A. M., Kennis, H. M. & Van Der Gulden, W. I. (1984) *Lab. Anim.* **18**, 106–109.
34. Ackerman, A. (1997) in *Histologic Diagnosis of Inflammatory Skin Diseases*, ed. Ackerman, A. (Williams & Wilkins, Baltimore), pp. 179–183.